The Astrophysical Journal Letters, 898:L52 (6pp), 2020 August 1 https://doi.org/10.3847/2041-8213/aba695

An Experimental Study of Chemical Desorption for Phosphine in Interstellar Ice

Thanh Nguyen[1], Yasuhiro Oba[1], Takashi Shimonishi[2,3], Akira Kouchi[1], and Naoki Watanabe[1]
[1] Institute of Low Temperature Science, Hokkaido University N19W8, Kita-ku, Sapporo, Hokkaido, 060-0819, Japan; oba@lowtem.hokudai.ac.jp
[2] Center for Transdisciplinary Research, Niigata University Ikarashi-ninocho 8050, Nishi-ku, Niigata, 950-2181, Japan
[3] Environmental Science Program, Department of Science, Faculty of Science, Niigata University Ikarashi-ninocho 8050, Nishi-ku, Niigata, 950-2181, Japan
Received 2020 May 26; revised 2020 July 15; accepted 2020 July 15; published 2020 August 3

Abstract

Phosphine (PH_3), an important molecule for the chemistry of phosphorus (P)-bearing species in the interstellar medium (ISM) is considered to form primarily on interstellar grains. However, no report exists on the processes of PH_3 formation on grains. Here, we experimentally studied the reactions of hydrogen (H) atoms and PH_3 molecules on compact amorphous solid water, with a particular focus on the chemical desorption of PH_3 at 10–30 K. After exposure to H atoms for 120 minutes, up to 50% of solid PH_3 was lost from the icy surface. On the basis of experiments using deuterium atoms, it was concluded that the loss of PH_3 resulted from chemical desorption through the reactions $PH_3 + H \rightarrow PH_2 + H_2$ and/or $PH_2 + H \rightarrow PH_3$. The effective desorption cross-section was $\sim 5 \times 10^{-17}$ cm^2, which is three times larger than that of hydrogen sulfide measured under similar experimental conditions. The present results suggest that the formation of PH_3, and possibly PH_2 and PH, followed by their desorption from icy grains, may contribute to the formation of PN and PO in the gas phase, and thus may play a role in the P chemistry of the ISM.

Unified Astronomy Thesaurus concepts: Dense interstellar clouds (371); Interstellar dust processes (838); Astrochemistry (75); Pre-biotic astrochemistry (2079)

1. Introduction

Phosphorus (P) chemistry in the interstellar medium (ISM) has attracted increasing attention from astrochemical communities. This is because P-bearing species such as nucleic acids and phospholipids are essential for life on Earth and have been detected in the ISM as PO and PN in recent decades (e.g., Turner et al. 1990; Agúndez et al. 2014; Fontani et al. 2016; Rivilla et al. 2020). Previous astronomical observations indicated the depletion of P-bearing species in the gas phase of the dense and cold ISM by a factor of $>10^2$ relative to the cosmic abundance of P (the missing phosphorus problem; Turner et al. 1990; Fontani et al. 2016; Lefloch et al. 2016). Such significant depletion suggests that the bulk of P-bearing species are locked on interstellar grains. In meteorites, phosphorus is identified as inorganic minerals such as schreibersite and hydroxyapatite (Fuchs 1969; Pasek & Lauretta 2005) and alkyl phosphonic acids (Cooper et al. 1992). However, to date no infrared observations of solid-state P-bearing species exist in any interstellar sources; hence, there is little information currently available about P chemistry on interstellar grains.

Modeling studies predict that phosphine (PH_3) is an important P-bearing species for the surface chemistry on interstellar grains (Charnley & Millar 1994; Aota & Aikawa 2012; Chantzos et al. 2020). The formation of PH_3 is not easy in the gas phase of the ISM (Millar 1991). Accordingly, PH_3 has been proposed to form via the following reactions on grains (Chantzos et al. 2020; Rivilla et al. 2020):

$$P + H \rightarrow PH, \quad \Delta H = -277 \text{ kJ mol}^{-1} \tag{1}$$

$$PH + H \rightarrow PH_2, \quad \Delta H = -347 \text{ kJ mol}^{-1} \tag{2}$$

$$PH_2 + H \rightarrow PH_3, \quad \Delta H = -326 \text{ kJ mol}^{-1}. \tag{3}$$

Because reactions (1)–(3) are barrierless, they can effectively proceed on grains, even at temperatures as low as 10 K where hydrogen (H) atoms can diffuse and encounter other species on the grain surface (Hama & Watanabe 2013). However, neither PH_3 nor other P-bearing species have been observed in a solid state, as noted earlier. Turner et al. (2015, 2018, 2019) experimentally studied the conversion of solid PH_3 into other chemical species such as diphosphane (P_2H_4), phosphoric acid, and methylphosphonic acid by the energetic processes applied to PH_3-containing ices at low temperatures.

In addition to its conversion into other species, PH_3 may also be lost from grains by desorption without decomposition. Because thermal desorption takes place at roughly 60 K (Turner et al. 2015), PH_3 may desorb during warming-up phases toward star formation even when formed at lower temperatures. Non-thermal desorption can, in principle, occur even at temperatures below its thermal desorption temperature, which can be further divided into two types of processes: desorption by energetic processes such as photon and ion bombardment, and non-energetic chemical (or reactive) desorption. The former utilizes photon or ion energy to cause desorption, and has been extensively studied experimentally involving various molecules such as water, carbon monoxide, and methanol (Öberg et al. 2009; Fayolle et al. 2011; Bertin et al. 2016; Cruz-Diaz et al. 2016). The latter, i.e., chemical desorption, has also been experimentally studied involving various species (Dulieu et al. 2013; He et al. 2017; Chuang et al. 2018). Because chemical desorption has a strong advantage in that it does not require any external energy, it can occur even in the dense and cold regions of the ISM, where external photons cannot penetrate. However, unlike energetic desorption processes, it is not easy to evaluate the efficiency of chemical desorption experimentally because of technical difficulties, giving rise to significant uncertainty for the quantification of its efficiency.

Recently, we were successful in quantifying the efficiency of chemical desorption using Fourier-transform infrared (FTIR)

spectroscopy (Oba et al. 2018). This method applies to specific reaction systems only, i.e., where the initial reactant is the same as the final product. We estimated the chemical desorption efficiency of hydrogen sulfide (H_2S) via the following successive H-abstraction and H-addition reactions:

$$H_2S + H \rightarrow HS + H_2, \quad \Delta H = -58 \text{ kJ mol}^{-1} \tag{4}$$

$$HS + H \rightarrow H_2S, \quad \Delta H = -374 \text{ kJ mol}^{-1} \tag{5}$$

where 60% of the initial solid H_2S was lost by chemical desorption with an effective desorption cross-section of 2×10^{-17} cm^2 (Oba et al. 2018, 2019). In the case of PH_3, the interaction with H atoms on grain surfaces may result in a similar scheme to that of H_2S as follows:

$$PH_3 + H \rightarrow PH_2 + H_2, \quad \Delta H = -106 \text{ kJ mol}^{-1}. \tag{6}$$

The produced PH_2 radical will further react with an additional H atom to again yield PH_3 via reaction (3). Because reaction (6) is exothermic with a moderate activation barrier of 14 kJ mol^{-1} (Yu et al. 1999), it is expected that reaction (6) can proceed via quantum tunneling at low temperatures. If reactions (6) and (3) proceed, they may induce chemical desorption of PH_3 and/or PH_2, as in the case with H_2S. So in this Letter, we present experimental results on the interactions of solid PH_3 with H atoms on icy surfaces at low temperatures to study the possible loss of PH_3 from icy surfaces by chemical desorption. The obtained results will be helpful for interpreting the abundance of PH_3 toward various astronomical sources, and will provide a better understanding of P chemistry in the ISM.

2. Experiments

All experiments were performed using the Apparatus for Surface Reaction in Astrophysics (ASURA) system. The ASURA system is described in previous studies (Watanabe et al. 2006; Nagaoka et al. 2007). In brief, the ASURA comprises a stainless-steel vacuum chamber with a basic pressure of 10^{-10} torr, multiple turbo molecular pumps, an aluminum (Al) reaction substrate attached to a closed-cycle helium cryostat, a quadrupole mass spectrometer (QMS), and an FTIR with an incident angle of 83° from the surface normal. The Al substrate was covered with amorphous silicates (Mg_2SiO_4) with a thickness of 10–30 nm, which were prepared by magnetron sputtering to sintered polycrystalline Mg_2SiO_4. The surface temperature was controlled between 5 and 300 K.

Chemical processes of PH_3 were surveyed on compact amorphous solid water (c-ASW), which was prepared by vapor deposition of H_2O via a capillary plate with an incident angle of 45° to the substrate and maintained at 110 K. The thickness of the c-ASW was estimated to be approximately 30 monolayers (ML; 1 ML = 1×10^{15} molecules cm^{-2}). The substrate was cooled to the reaction temperature (10–30 K). We anticipated the silicate surface to be fully covered with c-ASW under our experimental conditions, thereby indicating that all chemical reactions of PH_3 took place on the surface of the c-ASW.

Gaseous PH_3 was produced by the reaction of calcium phosphide (Ca_3P_2, 97%; Mitsuwa Chemicals Co., Ltd) with H_2O ($Ca_3P_2 + 6H_2O \rightarrow 2PH_3 + 3Ca(OH)_2$) in a separate vacuum chamber, followed by its cryogenic purification to remove by-products of the reaction such as P_2H_4 and molecular hydrogen (H_2) (Huang et al. 1977). The purified PH_3 gas was introduced through the same capillary plate onto the c-ASW layer at different temperatures (10, 20, and 30 K) to produce a solid PH_3 with a thickness of approximately 0.5 ML, which was estimated using the peak area of the P–H stretching band at 2320 cm^{-1} (Francia & Nixon 1973) with an absorption coefficient is 7.0×10^{-18} cm molecule^{-1} (Turner et al. 2015). The deposition rate of PH_3 was 1 ML minute^{-1}.

The H atoms were generated through the dissociation of H_2 in a microwave-discharged plasma in a Pyrex tube. The H atoms were cooled to 100 K before reaching the substrate by multiple collisions with the inner wall of the Al tube at 100 K (Nagaoka et al. 2007). Using the method of Oba et al. (2014), the flux of H atoms was estimated as 1.1×10^{13} atoms cm^{-2} s^{-1}. The deposited solid PH_3 was exposed to H atoms at each temperature for 120 minutes. Molecules on the surface were analyzed in situ using FTIR spectroscopy in the spectrum range of 4000–700 cm^{-1} at a resolution of 2 cm^{-1}. Reactants and products desorbed from the substrate were also monitored by the QMS via the temperature-programmed desorption (TPD) method with a ramping rate of 4 K minute^{-1}.

3. Results and Discussion

3.1. Loss of PH_3 by Reactions with H Atoms on Compact Amorphous Solid Water at Different Temperatures

Figure 1(a) shows the FTIR spectrum of solid PH_3 (0.5 ML) on c-ASW at 10 K. The inset shows an enlarged spectrum at 2250–2400 cm^{-1}. The PH_3 solid has mainly three bands in this region: 2320 cm^{-1} for the stretching band (highlighted in the inset) and 1107 and 985 cm^{-1} for the bending bands (Francia & Nixon 1973; Turner et al. 2015); however, the latter two peaks were not observed in Figure 1(a) due to their low absorption coefficients (Turner et al. 2015). Further deposition of PH_3 gas did not show any other peaks attributable to possible contaminants such as P_2H_4 (2294 and 1061 cm^{-1}; Turner et al. 2015), indicating that the purity of the PH_3 gas was sufficiently high for the present experiment.

Figure 1(b) displays variations in the difference spectra of PH_3 focusing on the P–H stretching region after exposure to H atoms for up to 120 minutes at 10 K, in addition to the initial spectrum for comparison. The intensity of the P–H stretching band was reduced with exposure to H atoms. In contrast, when solid PH_3 was exposed to H_2 molecules only under the same experimental conditions, the PH_3 decrease was negligible. In addition, PH_4 cannot form by the addition of H to PH_3 due to its endothermicity (Howell & Olsen 1976). Hence, a decrease in PH_3 should result from desorption triggered by reaction (6). PH_2 radicals formed by reaction (6) do not readily react with H_2O and H_2 at 10–30 K due to the endothermicity of each reaction. The formation of P_2H_4 may be possible if two PH_2 radicals are present nearby on the icy surface; however, under the present experimental conditions, where the surface coverage of PH_3 is much less than unity, its formation is less expected to occur. In fact, any traces relevant to other P-bearing species were not confirmed by the FTIR spectra. The loss of PH_3 was also confirmed via the TPD–QMS experiment. Figure 2 shows the TPD spectra of the PH_3 with and without exposure to H atoms at 10 K for 120 minutes. A single desorption peak was observed at roughly 68 K for both TPD spectra, which can be attributed to PH_3 desorbed from the surface of c-ASW. The TPD–QMS measurements showed that the loss of PH_3 was 50% at 10 K, which is in agreement with the estimation from the FTIR spectra (see Section 3.2). Desorption of all other P-bearing species such as P_2H_4 ($m/z = 66$) was not confirmed

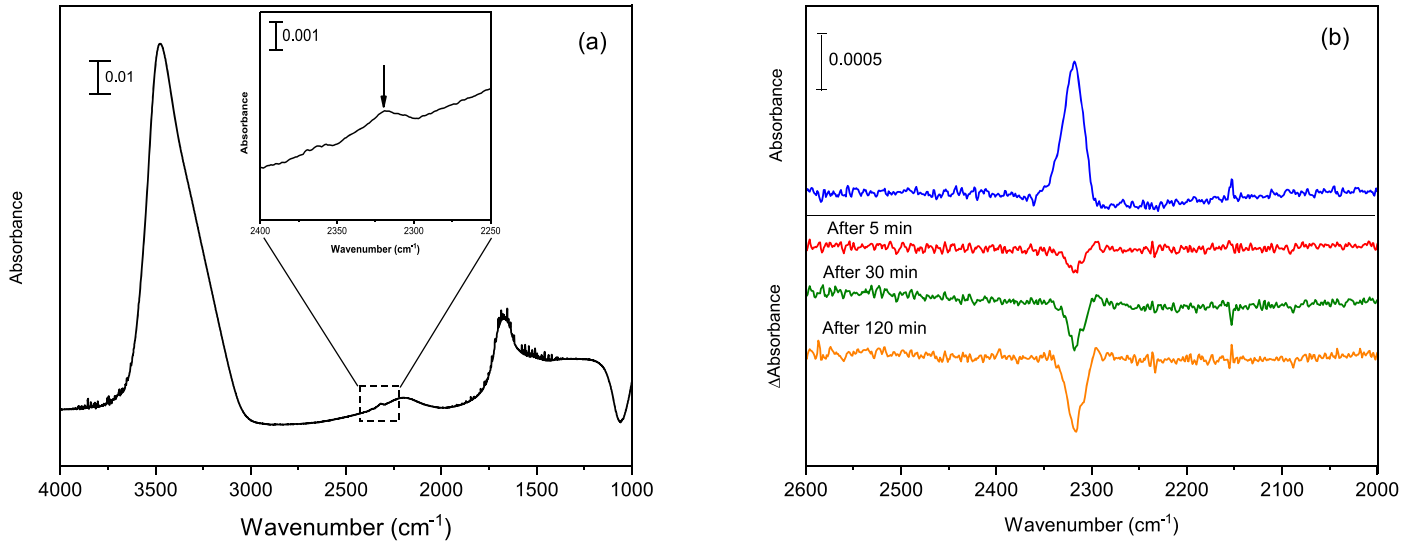

Figure 1. (a) Fourier-transform infrared profile of PH_3 on compact amorphous solid water (30 ML) at 10 K. The P–H stretching band region (2400–2250 cm^{-1}) is enlarged in the inset. The arrow indicates the P–H stretching band of solid PH_3 at 2320 cm^{-1}. (b) Variations in the difference spectra of solid PH_3 after exposure to H atoms for 5, 30, and 120 minutes at 10 K. The initial P–H stretching band is shown as a reference. The observed dip at 1050 cm^{-1} in (a) could be caused by the interaction of H_2O with silicates (Potapov et al. 2018).

during the TPD–QMS measurement. These results indicated that PH_3 was not converted to other P-bearing species but was lost from the substrate following interaction with H atoms.

To test the hypothesis that the loss of PH_3 occurred because of chemical desorption through reactions (6) and/or (3), we carried out an additional experiment in which solid PH_3 interacted with D atoms on c-ASW retained at 10 K. We anticipated that the following successive H-abstraction and D-addition reactions would proceed on the substrate, resulting in the formation of a singly deuterated phosphine (PH_2D):

$$PH_3 + D \rightarrow PH_2 + HD, \quad (7)$$

$$PH_2 + D \rightarrow PH_2D. \quad (8)$$

Figure 3 shows the FTIR spectra after exposure of PH_3 to D atoms for up to 120 minutes at 10 K. The P–H stretching band at 2320 cm^{-1} was reduced with atom exposure time and, simultaneously, a new peak appeared at 1686 cm^{-1}, representing the P–D stretching band of deuterated phosphine (Francia & Nixon 1973). In contrast, the P–D stretching band did not appear when the PH_3 solid was exposed to D_2 molecules only. These results indicate that PH_2D formed via reactions (7) and (8). Further deuteration would be possible; however, to investigate the process in more detail is beyond the scope of the present study. Therefore, in the reaction of PH_3 with H atoms, we concluded that reactions (6) and (3) proceeded, resulting in the loss of PH_3 from the surface of c-ASW by chemical desorption via reactions (6) and/or (3).

3.2. Quantification of the PH_3 Chemical Desorption

Figure 4 shows variations in the relative abundance of PH_3 after exposure to H atoms at 10, 20, and 30 K with relevance to atom exposure times. The loss of PH_3 was also observed at 20 and 30 K. Roughly 50%, 40%, and 30% of the initial PH_3 solid was lost after exposure to H atoms for 120 minutes at 10, 20, and 30 K, respectively. The observed desorption fraction variations based on temperature can be explained as described

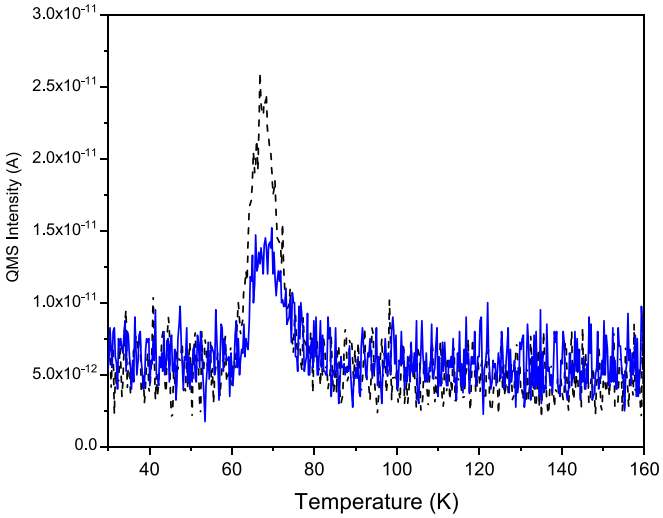

Figure 2. TPD spectra of the initial PH_3 without (dash black line; 0.5 ML) and with (solid blue line) exposure to H atoms on c-ASW maintained at 10 K.

in our previous paper (Oba et al. 2019). In brief, at higher temperatures such as 30 K, where most H atoms desorb immediately from the surface, the reaction causing chemical desorption will mainly take place at deeper absorption sites. Contrastingly, solid PH_3 adsorbed at shallower sites will be less likely to react with H atoms, which will suppress the desorption of PH_3 at higher temperatures.

By simply assuming that the chemical desorption proceeds through a single process (e.g., photodesorption), the variations in the relative abundance of PH_3 (Figure 4) can be fitted to a single exponential decay curve defined by

$$\frac{\Delta[PH_3]_t}{\Delta[PH_3]_0} = A \times (1 - \exp(-\sigma\varphi t)), \quad (9)$$

where $\Delta[PH_3]_0$ and $\Delta[PH_3]_t$ represent the abundance of PH_3 at time = 0 and t, respectively, A is a saturation value for the

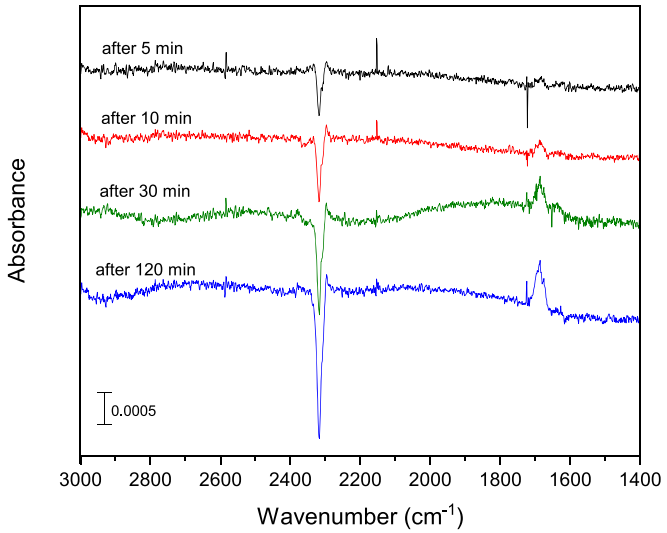

Figure 3. Variations in the difference spectra of the PH_3 (2.5 ML) after exposure to D atoms for 5 minutes (black curve), 10 minutes (red curve), 30 minutes (green curve), and 120 minutes (blue curve) on c-ASW maintained at 10 K.

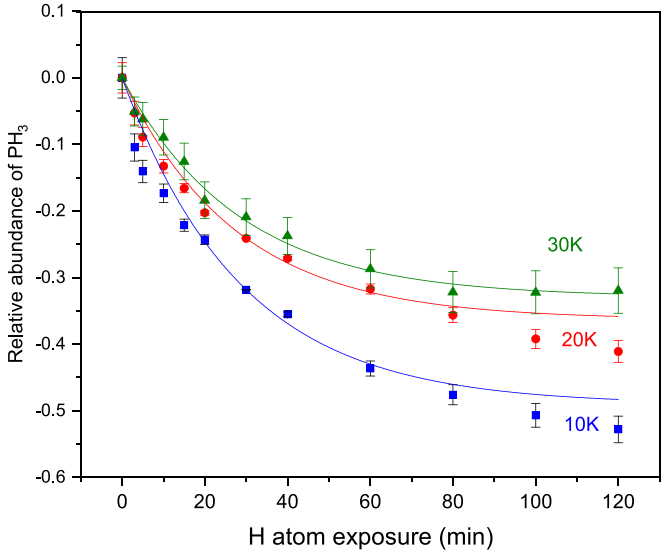

Figure 4. Variations in the relative abundance of PH_3 on c-ASW as a function of the H atom exposure time at 10 K (blue squares), 20 K (red circles), and 30 K (green triangles).

desorption fraction of PH_3, σ is the effective cross-section of chemical desorption in cm^2, and φ represents the flux of H atoms (1.1×10^{13} atoms cm^{-2}). By fitting the plots in Figure 4 into Equation (9) we obtained the effective desorption cross-section at each temperature: $(5.3 \pm 0.5) \times 10^{-17}$ cm^2 at 10 K, $(5.6 \pm 0.5) \times 10^{-17}$ cm^2 at 20 K, and $(5.4 \pm 0.5) \times 10^{-17}$ cm^2 at 30 K. Note that the obtained effective cross-section can be considered as the lower limit of the actual cross-section because most of the impinged H atoms will be consumed by H–H recombination before interacting with PH_3. The obtained effective cross-section appeared to show little dependence on temperature, as in the case of the chemical desorption of H_2S (Oba et al. 2019). However, the values of the effective cross-section derived from Equation (9) are likely to have been underestimated, particularly at higher temperatures, where H atoms should contribute less to surface reactions (as explained earlier in this section). Hence, it should be considered that the actual efficiency of chemical desorption per reactive event should increase with temperature. Unfortunately, desorption efficiency for each reaction (i.e., reactions (3) and (6)) could not be determined under the present experimental conditions; nonetheless, some modeling studies have assumed that no desorption occurred in the case of two-product reactions (i.e., reaction (6)) (Garrod et al. 2007). Further studies are thus necessary for elucidating the chemical desorption of PH_3.

The obtained effective desorption cross-section (5.3×10^{-17} cm^2) was larger by a factor of 3 than that for H_2S obtained under similar experimental conditions (1.6×10^{-17} cm^2; Oba et al. 2019), despite the thermodynamic parameters for each reaction system being similar to one another (Table 1). According to Garrod et al. (2007), the desorption probability and fraction are constrained by multiple parameters including the heat of the reaction; hence, there may be other parameters besides the reaction to heat that can cause a large difference. Recent theoretical studies focused on new factors such as energy dissipation upon chemical reactions and the adsorption state of molecules on surfaces, thus extending the discussion regarding the efficiency of chemical desorption in more detail (Fredon et al. 2017; Korchagina et al. 2017; Fredon & Cuppen 2018; Kayanuma et al. 2019; Pantaleone et al. 2020). To elucidate why PH_3 is more effectively desorbed than H_2S is beyond the scope of the present study. We believe a combination of experiments and computational calculations is necessary to fully understand chemical desorption in dense clouds.

4. Astrophysical Implications

PH_3 has been astronomically observed in the circumstellar envelope of a carbon star, IRC +10216 (e.g., Agúndez et al. 2014). Alongside other P-hydrides (PH and PH_2), it has never been detected in the dense and cold regions of the ISM, where only PO and PN have to date been found as P-bearing species (Fontani et al. 2016; Lefloch et al. 2016). Modeling studies of phosphorus chemistry in star-forming regions predict that PH_3 could be a major molecular reservoir of P-bearing species in ice mantles (Charnley & Millar 1994; Aota & Aikawa 2012; Chantzos et al. 2020). In relatively diffuse clouds (<5 mag), solid PH_3 is thought to desorb mainly due to the photodesorption by interstellar UV photons (Chantzos et al. 2020). In a protostellar envelope, mapping observations of PN and PO suggest that PH_3 would be released from grains into the gas phase by protostellar shocks (Rivilla et al. 2020). However, little is known about the desorption of PH_3 from grains in quiescent and dense molecular clouds without prominent star formation activity. Our experimental study of chemical desorption suggests the presence of PH_3 gas (and possibly PH_2) in the dense, cold, and quiescent regions of molecular clouds, if reactions (1)–(3) take place on grains.

Following the method of Oba et al. (2019), we estimate the desorption efficiency of PH_3 per incident H atom to be 2.3% based on the present results. If the PH_3 desorbed via reaction (3) only, the desorption efficiency would be doubled. This is a lower limit on the desorption efficiency per reactive event, since a considerable amount of incident H atoms will be used for recombination into H_2. Astrochemical simulations involving grain surface chemistry of P-bearing molecules assume 1% for the desorption efficiency per reactive event (Chantzos et al. 2020).

Table 1
Summary of the Heat of Reaction (ΔH), Activation Energy (E_a), Binding Energy with H_2O, and Effective Cross-section Determined in the Present Experiment

	$PH_3 + H \rightarrow PH_2 + H_2$	$PH_2 + H \rightarrow PH_3$	$H_2S + H \rightarrow HS + H_2$	$HS + H \rightarrow H_2S$
ΔH (kJ mol^{-1})	−106	−326	−58	−374
E_a (kJ mol^{-1})	13.6[a]	0	12.6[b]	0
	PH_2	PH_3	HS	H_2S
Binding energy with H_2O (kJ.mol^{-1})	n.a.[c]	10.5–12.7[d]	8.8[e]	16.1[e]
Effective cross-section (cm^2)	$(5.3 \pm 0.5) \times 10^{-17}$		$(1.6 \pm 0.2) \times 10^{-17}$	

Notes.
[a] Yu et al. (1999).
[b] Lamberts & Kästner (2017).
[c] Not available from the literature.
[d] Dissociation energy of the PH_3–H_2O complex (Viana & da Silva 2015).
[e] When no dangling H of H_2S and HS is present in the structure (Oba et al. 2018).

The efficiency is, however, much lower than the value estimated in the present study, and thus needs to be updated. In addition, the implementation of the surface H-abstraction reaction for PH_3 in the modeling can further enhance its chemical desorption. Future astrochemical simulations with updated chemical desorption efficiency and surface reaction network of P-bearing species, along with astronomical observations of PH_3 toward quiescent dense cores such as TMC-1, are required for comprehensive understanding of the missing phosphorus problem in star-forming regions.

After the desorption, PH_3 may be destroyed by a series of processes such as photolysis and H-abstraction (e.g., reaction (6) in the gas phase), followed by the formation of PN and PO via the following reactions:

$$PH + N \rightarrow PN + H, \quad (10)$$

$$PH + O \rightarrow PO + H. \quad (11)$$

Because PH is an important precursor for PN and PO in the gas phase (Charnley & Millar 1994), the formation of PH is also a key process that requires in-depth understanding as it relates to P-bearing chemistry in the ISM.

In addition to PH_3 and PH_2, PH could also be desorbed from grains by chemical desorption during reaction (1) in dense, cold clouds. Note that the formation of PH from PH_3 via photolysis may not be efficient in such regions where the ultraviolet field is very weak (Prasad & Tarafdar 1983). In addition, H-abstraction from PH_3, which requires sufficient energy to overcome a moderate activation barrier (e.g., reaction 6), will not effectively proceed by quantum tunneling in the gas phase at the typical temperatures of dense clouds (∼10 K). Hence, chemical desorption of PH from grains by reaction (1) may present the most promising pathway for the possible presence of PH in the gas phase of dense, cold clouds. The formed PH can potentially be further used for the formation of PN and PO through reactions (10) and (11), respectively, even in such cold regions. Unfortunately, we could not estimate the efficiency of chemical desorption by reaction (1) in the present study. However, if PH can desorb upon formation at an efficiency comparable with or higher than PH_3 via reaction (3), the aforementioned hypothesis becomes plausible. Because the present study provides promising results on the presence of P-hydrides as a gas and/or solid in various astronomical sources, additional observation of P-hydrides is anticipated in the future.

The authors thank K. Furuya at NAOJ for his advice on phosphorus chemistry in the ISM. The authors also thank W. M. C. Sameera at Hokkaido University for discussion on the binding energy of P species with H_2O. This work is partly supported by JSPS KAKENHI grant Nos. JP17H06087, JP17H04862, and JP19K23449.

ORCID iDs

Thanh Nguyen https://orcid.org/0000-0003-3788-5992
Yasuhiro Oba https://orcid.org/0000-0002-6852-3604
Takashi Shimonishi https://orcid.org/0000-0002-0095-3624
Akira Kouchi https://orcid.org/0000-0002-0495-5408
Naoki Watanabe https://orcid.org/0000-0001-8408-2872

References

Agúndez, M., Cernicharo, J., Decin, L., Encrenaz, P., & Teyssier, D. 2014, ApJL, 790, L27
Aota, T., & Aikawa, Y. 2012, ApJ, 761, 74
Bertin, M., Romanzin, C., Doronin, M., et al. 2016, ApJL, 817, L12
Chantzos, J., Rivilla, V. M., Vasyunin, A., et al. 2020, A&A, 633, A54
Charnley, S. B., & Millar, T. J. 1994, MNRAS, 270, 570
Chuang, K. J., Fedoseev, G., Qasim, D., et al. 2018, ApJ, 853, 102
Cooper, G. W., Onwo, W. M., & Cronin, J. R. 1992, GeCoA, 56, 4109
Cruz-Diaz, G. A., Martín-Doménech, R., Muñoz Caro, G. M., & Chen, Y. J. 2016, A&A, 592, A68
Dulieu, F., Congiu, E., Noble, J., et al. 2013, NatSR, 3, 1338
Fayolle, E. C., Bertin, M., Romanzin, C., et al. 2011, ApJL, 739, L36
Fontani, F., Rivilla, V. M., Caselli, P., Vasyunin, A., & Palau, A. 2016, ApJL, 822, L30
Francia, M. D., & Nixon, E. R. 1973, JCP, 58, 1061
Fredon, A., & Cuppen, H. M. 2018, PCCP, 20, 5569
Fredon, A., Lamberts, T., & Cuppen, H. M. 2017, ApJ, 849, 125
Fuchs, L. H. 1969, in Meteorite Research, Astrophysics and Space Science Library, Vol. 12, ed. P. M. Millman (Dordrecht: Reidel), 683
Garrod, R. T., Wakelam, V., & Herbst, E. 2007, A&A, 467, 1103
Hama, T., & Watanabe, N. 2013, ChRv, 113, 8783
He, J., Emtiaz, S. M., & Vidali, G. 2017, ApJ, 851, 104
Howell, J. M., & Olsen, J. F. 1973, JAChS, 98, 7199
Huang, T.-H., Decius, J., & Nibler, J. 1977, JPCS, 38, 897
Kayanuma, M., Shoji, M., Furuya, K., et al. 2019, JPCA, 123, 5633
Korchagina, K. A., Spiegelman, F., & Cuny, J. 2017, JPCA, 121, 9485
Lamberts, T., & Kästner, J. 2017, JCPA, 121, 9736
Lefloch, B., Vastel, C., Viti, S., et al. 2016, MNRAS, 462, 3937
Millar, T. J. 1991, A&A, 242, 241
Nagaoka, A., Watanabe, N., & Kouchi, A. 2007, JPCA, 111, 3016
Oba, Y., Osaka, K., Watanabe, N., Chigai, T., & Kouchi, A. 2014, FaDi, 168, 185
Oba, Y., Tomaru, T., Kouchi, A., & Watanabe, N. 2019, ApJ, 874, 124
Oba, Y., Tomaru, T., Lamberts, T., Kouchi, A., & Watanabe, N. 2018, NatAs, 2, 228

Öberg, K. I., Linnartz, H., Visser, R., & van Dishoeck, E. F. 2009, ApJ, 693, 1209
Pantaleone, S., Enrique-Romero, J., Ceccarelli, C., et al. 2020, ApJ, 897, 56
Pasek, M. A., & Lauretta, D. S. 2005, AsBio, 5, 515
Potapov, A., Mutschke, H., Seeber, P., Henning, T., & Jäger, C. 2018, ApJ, 861, 84
Prasad, S. S., & Tarafdar, S. P. 1983, ApJ, 267, 603
Rivilla, V. M., Drozdovskaya, M. N., Altwegg, K., et al. 2020, MNRAS, 492, 1180
Turner, A. M., Abplanalp, M. J., Bergantini, A., et al. 2019, SciA, 5, eaaw4307
Turner, A. M., Abplanalp, M. J., Chen, S. Y., et al. 2015, PCCP, 17, 27281
Turner, A. M., Bergantini, A., Abplanalp, M. J., et al. 2018, NatCo, 9, 1
Turner, B. E., Tsuji, T., Bally, J., Guelin, M., & Cernicharo, J. 1990, ApJ, 365, 569
Viana, R. B., & da Silva, A. B. 2015, Comput. Theor. Chem., 1059, 35
Watanabe, N., Nagaoka, A., Hidaka, H., et al. 2006, P&SS, 54, 1107
Yu, X., Li, S.-M., Liu, J.-Y., et al. 1999, JPCA, 103, 6402